



Analysis of Rockburst Characteristics in Drilled-Blasted Horseshoe Tunnel Sections with Different Surrounding Rock Categories

Yong Xia^{1,2,a}, Haohan Xiao^{3,b}, Bo Sun^{1,2,c}, Hongtao Yu^{3,d*}

¹PowerChina Chengdu Engineering Corporation Limited, Chengdu, China

²Technological Innovation Center of Hydropower, Wind, Solar and Energy Storage of Tibet Autonomous Region, Tibet, China

³State Key Laboratory of Basin Water Cycle Simulation and Regulation, China Institute of Water Resources and Hydropower Research, Beijing, China

^a1990046@chidi.com.cn, ^bxiaohh@iwhr.com, ^ctjudamer@126.com, ^dyhtyhtsky2022@163.com

*Corresponding author

Abstract. With the deepening development of underground space, the issue of rockbursts in tunnel engineering has become increasingly prominent, severely affecting construction safety. This study employs numerical simulations, and experimental testing methods to investigate the rockburst characteristics in drilled-blasted tunnels under different surrounding rock categories. The results indicate that rockburst energy is primarily concentrated around the crown, the invert, and the surrounding rock near the tunnel walls. The initial support is within the limit bearing capacity range, and no damage to the initial support was observed due to rockbursts. Based on these findings, measures to strengthen rockburst monitoring and inspection are proposed. This research provides valuable theoretical and practical guidance for the prediction, prevention, and control of rockbursts in tunnel engineering.

Keywords: Tunnel Rock Burst, Numerical Simulation, Drilling and Blasting Method, Characteristics of Rock Bursts, Tunnel Support

1 Introduction

Tunnel engineering plays a crucial role in the development and utilization of underground space, serving as an indispensable component in key areas such as urban transportation, water conservancy facilities, and energy infrastructure^[1]. The phenomenon of rockbursts, as a frequent geological hazard, poses a serious threat to the safety and progress of tunnel construction. Therefore, an in-depth investigation into the characteristics and stress mechanisms of rockbursts is particularly urgent^[2]. For instance, in 2022, the Baihetan Hydropower Station project on the Yangtze River also experienced rock bursts during construction, resulting in substantial economic losses^[3]. Furthermore, in 2021, the construction of the G60 Hukun Expressway Tunnel faced delays due to rock

© The Author(s) 2025

Y. Qiu et al. (eds.), *Proceedings of the 2024 7th International Conference on Civil Architecture, Hydropower and Engineering Management (CAHEM 2024)*, Advances in Engineering Research 256, https://doi.org/10.2991/978-94-6463-650-5_49

bursts, prompting the construction team to reassess the support design for the surrounding rock and increase both the budget and project timeline^[4].

Many researchers focus on rockburst issues to enhance tunnel construction safety and efficiency. They utilize a combination of numerical simulations^[5], theoretical analyses^[6], and experimental testing^[7] to investigate the frequency, magnitude, spatial distribution, and other characteristics of rockbursts^[8]. These studies explore the decisive factors and mechanical mechanisms behind rockbursts in various surrounding rock conditions^[9], providing a solid theoretical foundation for their prediction, prevention, and control. Innovative research is also directed toward developing monitoring technologies, employing advanced techniques such as seismic monitoring and strain sensors for real-time monitoring of rock deformation and stress, which aids in predicting and mitigating rockburst events^[10]. Additionally, researchers investigate effective engineering measures, including optimizing support designs and strengthening construction management, to reduce rockburst risks. Despite significant advancements, existing research lacks specific critiques and discussions on limitations^[11]. For example, the accuracy of numerical simulations can be affected by model assumptions, while experimental tests may face scale constraints. Moreover, there is insufficient investigation into rockburst characteristics under certain conditions, and current monitoring technologies may lack the necessary sensitivity for effective prediction. Future research should address these gaps by exploring new materials and developing more complex rock behavior models to deepen the understanding of rockbursts^[12].

The objective of this paper is to thoroughly investigate the characteristics of rockbursts in drilled-blasted tunnels under different surrounding rock categories, along with a stress analysis to comprehensively study the impact of rockbursts on tunnel excavation projects^[13]. Through systematic observation and analysis of rockburst characteristics under varying surrounding rock conditions, this study aims to reveal the regularity of rockburst occurrences and, in conjunction with practical engineering scenarios^[14], propose technical recommendations for the prevention and control of rockbursts in drilled-blasted tunnels across different surrounding rock categories.

2 Implementation of Numerical Simulation for Drilled-Blasted Horseshoe Tunnel Construction

Based on the tunnel drilling and blasting method for a certain water conveyance tunnel, and considering the rock type, surrounding rock category, and burial depth, a rock burst analysis was conducted on typical tunnel sections 62+280 and 58+560. Different geometric models were adopted for sections of Class II and Class III surrounding rock. Please refer to Figure 1 for details.

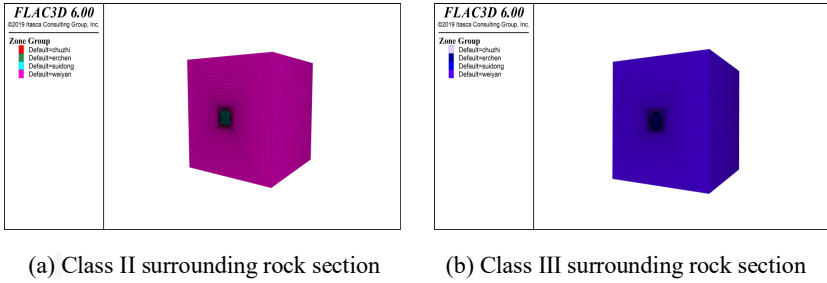


Fig. 1. Numerical Model of the Drilling and Blasting Tunnel Section

The model dimensions for both the Class II and Class III surrounding rock sections are 60×60×60 (length × width × height). The rock is represented as an elasto-plastic material with a yield criterion based on the Mohr-Coulomb criterion. Constraints are applied in the Z direction at the model's bottom, in the X direction on the outer surfaces, and in the Y direction along the tunnel axis. Initial stress is integrated using the Fish programming language, based on inverse analysis of the initial ground stress under the tunnel's environmental conditions. Normal stress is applied to the model's upper surface (Z-axis).

A composite support lining structure includes primary support with rock bolts, mesh reinforcement, shotcrete, and steel arch frames, while the secondary lining consists of cast-in-place reinforced concrete. Following the support lining for the drilling and blasting tunnel, the internal tunnel profile dimension is 7.5 m. Excavation dimensions are based on the combined shotcrete, cast-in-place concrete lining, and internal diameter, resulting in a horseshoe-shaped cross-section. Specific parameters are listed in Table 1.

Table 1. Support Lining Parameters for Drilling and Blasting Section

Tunnel Category	Primary Support Parameters	Secondary Lining Parameters
Class II Surrounding Rock	Excavation dimensions 9.20×9.07 m (width × height); 120 mm thick C30 shotcrete on the arch, local $\phi 10@200 \times 200$ mm rebar mesh, $\phi 25@1500 \times 1500$ mm system mortar rock bolts in a staggered arrangement, L=3.5 m in the 180° arch range	40 cm thick arch and 51–60 cm thick C40 reinforced concrete base, single-layer reinforcement
Class III Surrounding Rock	Excavation dimensions 9.26×9.10 m (width × height); 150 mm thick C30 shotcrete on the arch, $\phi 10@200 \times 200$ mm rebar mesh, $\phi 25@1500 \times 1500$ mm system mortar rock bolts in a staggered arrangement, with HW150×150 steel arch frames as needed	40 cm thick arch and 51–60 cm thick C40 reinforced concrete base, single-layer reinforcement

The excavation of the drilling and blasting tunnel is treated as a continuous tunneling process, with a simulation that replicates the step-by-step procedure. The specific steps are as follows:

- (1) The numerical analysis model reads the regressed ground stress field using the Fish language function to calculate the stress equilibrium state.

(2) For both Class II and Class III surrounding rock sections, excavation advances 3 m along the tunnel axis each time.

(3) After completing 2 excavation steps for Class II and 3 for Class III, shotcrete and rock bolts are applied.

(4) The simulation continues until the face advances 30 m, using custom language commands for automated control of all steps.

3 Application in Engineering

3.1 Project Overview

The hydraulic tunnel spans 69.204 km, comprising 29.022 km of soft rock and 40.182 km of hard rock. It experiences high horizontal ground stress, risking rock mass failure, spalling, and block falls. Some sections also face mild to moderate rock burst issues. This study focuses on constructing Class II and Class III surrounding rocks using the drilling and blasting method. The segment at 62+280, at a depth of 610 m, is mainly Class II rock, featuring medium to fine-grained granite. The segment at 59+690, at 1240 m depth, consists primarily of Class III rock, characterized by granodiorite similar to porphyritic biotite granite.

3.2 Characteristics of Rock Bursts and Support Stress Analysis in Class II Surrounding Rock

Analysis of Rock Burst Characteristics. The distribution of rock burst energy following the drilling and blasting construction is illustrated in Figure 2. When the tunnel excavation reaches $y = 30$ m, the rock burst energy in front of the face is minimal. The energy distribution is primarily concentrated within the rock mass ranging from 0.32 m in front of the face to 2.65 m behind it, with a depth along the tunnel circumference reaching up to 0.35 m. The maximum energy recorded is 36.1 kJ.

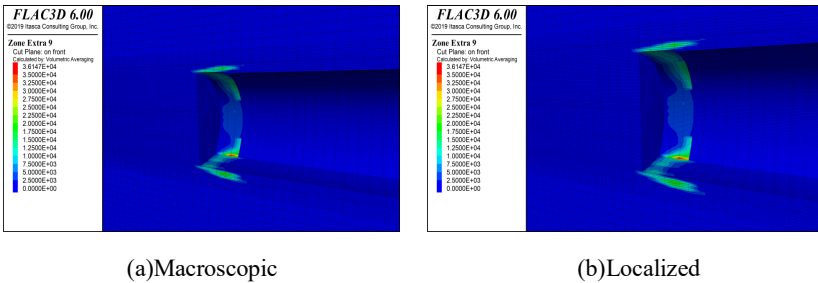


Fig. 2. Energy Distribution of Rock Bursts in Class II Surrounding Rock

Support Stress Analysis. After the initial support structure is applied during the excavation of the tunnel using the drilling and blasting method, the maximum compressive stress on the initial support is 6.22 MPa, primarily concentrated near the initial support's

vicinity. Notable tensile stress concentrations are observed near the bottom and top of the initial support, with a maximum tensile stress of 0.38 MPa, as shown in Figure 3.

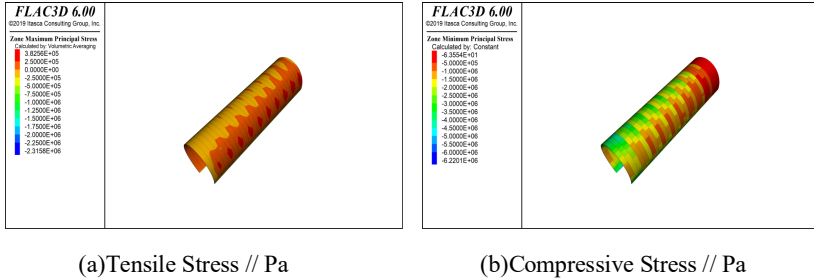


Fig. 3. Stress Distribution of Initial Support Structure in Class I Surrounding Rock / Pa

3.3 Study on Rock Burst Characteristics and Support Stress of Class III Surrounding Rock

Analysis of Rock Burst Characteristics. The distribution of rock burst energy following the drilling and blasting construction is illustrated in Figure 4. When the tunnel excavation reaches $y = 34.2$ m, the rock burst energy is primarily concentrated within the rock mass ranging from 0.65 m in front of the face to 4.6 m behind it, with a depth along the tunnel circumference reaching up to 1.74 m. The maximum energy recorded is 40.6 kJ.

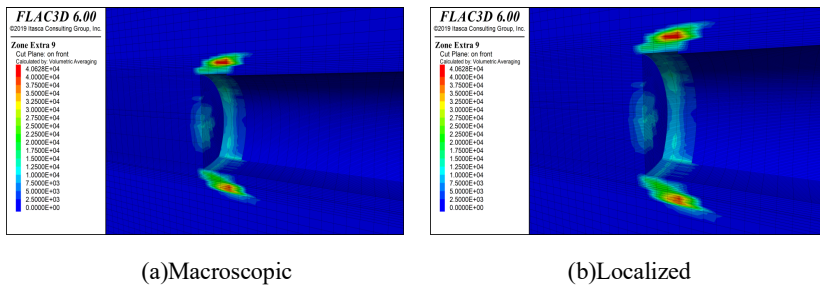


Fig. 4. Rock Burst Energy Distribution Map

Support Stress Analysis. After the initial support structure is applied during the excavation of the tunnel using the drilling and blasting method, the maximum compressive stress on the initial support is 14.2 MPa, primarily concentrated near the top of the initial support. Significant tensile stress concentrations are observed near the two sides and the top of the initial support, with a maximum tensile stress of 0.55 MPa. Please refer to Figure 5 for details.

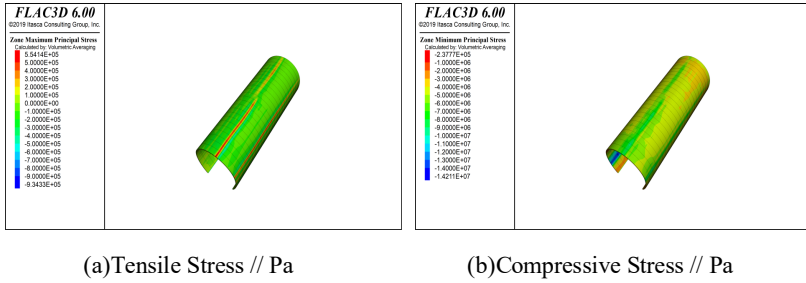


Fig. 5. Stress Distribution of Initial Support Structure / Pa

4 Recommendations for Rock Burst Prevention and Control Technologies in Drilling and Blasting Tunnel

Numerical calculations of rock burst patterns for KM drilling and blasting tunnels show that segments 62+280 and 59+690 are moderate rock burst areas. Rock burst energy is concentrated near the crown, invert, and surrounding rock, with a maximum depth of 4.38 m behind the face, and a smaller distribution of 0.32 to 2.1 m in front. The initial support's compressive and tensile stresses are within safe limits, showing no damage from rock bursts. Energy tends to accumulate before excavation and after initial support is applied.

To address moderate rock bursts, enhanced on-site monitoring is recommended. Real-time monitoring helps predict occurrences and assess intensity, forming the basis for control measures. Strengthening on-site observations during construction is also crucial for early detection of rock burst signs.

Table 2. Statistical Table of Rock Burst Energy and Support Stress for Various Surrounding Rock Categories in Drilling and Blasting Method

Stake Number	Environmental Condition	Maximum Compressive Stress of Concrete / MPa	Allowable Compressive Stress / MPa	Maximum Tensile Stress of Concrete / MPa	Allowable Tensile Stress / MPa	Rock Burst Radiation Energy / kJ	Rock Burst Level
62+280	Class II + Depth 610 m	6.22	14.3	0.38	1.43	36.1	Moderate Rock Burst
59+690	Class III + Depth 1240 m	14.2	14.3	0.55	1.43	40.6	Moderate Rock Burst

5 Conclusion

Rock bursts are disasters that occur in high geostress environments when the surrounding rock suddenly fractures due to exceeding its strength, releasing energy. This study analyzes the characteristics of rock bursts in drilling and blasting tunnels under different surrounding rock categories, leading to the following conclusions:

(1) Distribution of Rock Burst Energy: The energy is primarily concentrated near the crown, invert, and surrounding rock of the tunnel, with a maximum depth of 4.38 m behind the face, and a small amount is distributed in the surrounding rock in front of the face.

(2) State of Initial Support Stress: Both the compressive and tensile stresses of the initial support are within the limits of bearing capacity. After the application of initial support, rock bursts have not caused damage to the initial support, with energy accumulation observed at positions prior to excavation and after the initial support application.

(3) Recommendations for Prevention and Control Measures: For moderate rock burst sections, it is advisable to enhance on-site monitoring. During construction, it is also essential to strengthen observations and inspections to promptly detect signs of rock bursts.

Acknowledgments

This research was funded by the Science and Technology Major Project of Xizang Autonomous Region during the 14th Five-Year Plan Period. (Science and Technology Major Project of Xizang Autonomous Region of China (XZ202201ZD0003G)).

References

1. Yu Y, Geng D, Tong L, et al. Time fractal behavior of microseismic events for different intensities of immediate rock bursts[J]. *International Journal of Geomechanics*, 2018, 18(7): 06018016.
2. Shui G H, Yao J M, Yan Y Y, et al. Danger assessment of rock burst base on damage theory and its application[J]. *Disaster Advances*, 2010, 3(4):258-261.
3. Di Y, Wang E, Li Z, et al. Comprehensive Early Warning Method of Microseismic, Acoustic Emission and Electromagnetic Radiation Signals of Rock Burst Based on Deep Learning[J]. *SSRN Electronic Journal*, 2023.
4. Du L J, Hong K, Wang J X, et al. Characteristics and Control Technologies of Rock Bursts during TBM Construction in Deep-Buried Tunnels[J]. *Tunnel Construction (Chinese and English)*, 2021, 41(01): 1-15.
5. Hu J, Wang Y, Ma Z, et al. Experimental and Numerical Analysis of Rock Burst Tendency and Crack Development Characteristics of Tianhu Granite[J]. *Geofluids*, 2021.
6. Zhang D X, Guo W Y, Zang C W, et al. A new burst evaluation index of coal-rock combination specimen considering rebound and damage effects of rock[J]. *Geomatics, Natural Hazards and Risk*, 2020, 11(1):984-999.

7. Wu Y Z, Gao F Q, Chen J Y, et al. .Experimental Study on the Performance of Rock Bolts in Coal Burst-Prone Mines[J].Rock Mechanics and Rock Engineering, 2019, 52(10).
8. Wu S, Yan Q, Tian S H W. Prediction of rock burst intensity based on multi-source evidence weight and error-eliminating theory[J]. Environmental Science and Pollution Research, 2023, 30(29):74398-74408.
9. Wu Z, Pan P Z, Chen J, et al. Mechanism of Rock Bursts Induced by the Synthetic Action of "Roof Bending and Rock Pillar Prying" in Subvertical Extra-Thick Coal Seams[J]. Frontiers in Earth Science, 2021.
10. Lin M D, Yao D J, Anye C, et al. Monitoring and pre-warning of rockburst hazard with technology of stress field and wave field in underground coalmines[J]. Chinese Journal of Rock Mechanics and Engineering, 2017.
11. Chambers D, Shragge J. Seismoacoustic Monitoring of a Longwall Face Using Distributed Acoustic Sensing[J]. Bulletin of the Seismological Society of America, 2023.
12. Wang Y, Xu J, Xu J, et al. Estimation of Rock Burst Grades Using Rock Mass Strength[J]. Advances in Civil Engineering, 2020.
13. Xiao H, Cao R, Feng S. Intelligent Attitude Control Method for Shield Tunneling Machines Considering a Rectifying Mechanism: A Case Study of the Chengdu Subway[J]. International Journal of Geomechanics, 2024, 24(8): 05024006.
14. Xiao H, Chen Z, Cao R, et al. Prediction of shield machine posture using the GRU algorithm with adaptive boosting: A case study of Chengdu Subway project[J]. Transportation Geotechnics, 2022, 37: 100837.

Open Access This chapter is licensed under the terms of the Creative Commons Attribution-NonCommercial 4.0 International License (<http://creativecommons.org/licenses/by-nc/4.0/>), which permits any noncommercial use, sharing, adaptation, distribution and reproduction in any medium or format, as long as you give appropriate credit to the original author(s) and the source, provide a link to the Creative Commons license and indicate if changes were made.

The images or other third party material in this chapter are included in the chapter's Creative Commons license, unless indicated otherwise in a credit line to the material. If material is not included in the chapter's Creative Commons license and your intended use is not permitted by statutory regulation or exceeds the permitted use, you will need to obtain permission directly from the copyright holder.

